PHYSICAL REVIEW A **74**, 042718 (2006)

Differential cross sections for muonic atom scattering from hydrogenic molecules

Andrzej Adamczak*
Institute of Nuclear Physics, Polish Academy of Sciences, 31-342 Kraków, Poland
and Rzeszów Technical University, 35-959 Rzeszów, Poland

(Received 8 August 2006; published 18 October 2006)

The differential cross sections for low-energy muonic hydrogen atom scattering from hydrogenic molecules are directly expressed by the corresponding amplitudes for muonic atom scattering from hydrogen-isotope nuclei. The energy and angular dependence of these three-body amplitudes is thus taken naturally into account in scattering from molecules, without involving any pseudopotentials. Effects of the internal motion of nuclei inside the target molecules are included for every initial rotational-vibrational state. These effects are very significant as the considered three-body amplitudes often vary strongly within the energy interval $\lesssim 0.1$ eV. The differential cross sections, calculated using the presented method, have been successfully used for planning and interpreting many experiments in low-energy muon physics. Studies of μ^- nuclear capture in $p\mu$ and the measurement of the Lamb shift in $p\mu$ atoms created in H_2 gaseous targets are recent examples.

DOI: 10.1103/PhysRevA.74.042718 PACS number(s): 34.50.−s, 36.10.Dr

I. INTRODUCTION

A calculation of the differential cross sections for low-energy scattering of muonic hydrogen atoms from hydrogen-isotope (hydrogenic) molecules is the main subject of this paper. The cross sections are expressed in terms of the corresponding amplitudes for muonic atom scattering from hydrogen-isotope nuclei. Thus, a dependence of these three-body scattering amplitudes on the collision energy, scattering angle, and spin is directly included. For numerical calculations, the three-body amplitudes computed using the adiabatic method [1–8] are employed.

Many experiments in low-energy muon physics are performed using molecular hydrogen-isotope targets (see, e.g., Refs. [9–15]). For planning and interpreting such experiments, the differential cross sections for the following processes are often required:

$$\text{elastic scattering:} \quad a\mu(F) + BC \to a\mu(F) + BC, \tag{1a}$$

$$\text{isotopic exchange:} \quad a\mu + BC \to b\mu + AC, \tag{1b}$$

$$\text{and spin flip:} \quad a\mu(F) + AB \to a\mu(F') + AB. \tag{1c}$$

A monic hydrogen-isotope atom in the $1S$ state is denoted here by $a\mu$ or $b\mu$; F and F' stand for the initial and final total spin of the muonic atom. The molecules BC, AC, and AB denote the hydrogenic molecules H_2, D_2, T_2, HD, HT, or DT. The processes (1) can take place with simultaneous rotational and vibrational transitions in a target molecule. Thus, the name "elastic" assigned here to the scattering (1a) refers solely to the state of the muonic atom. The cross sections for the processes (1) are henceforth called the "molecular" cross sections.

For many years, only the cross sections for muonic hydrogen atom scattering from hydrogen-isotope nuclei ("nuclear" cross sections) were available:

$$\text{elastic scattering:} \quad a\mu(F) + b \to a\mu(F) + b, \tag{2a}$$

$$\text{isotopic exchange:} \quad a\mu + b \to b\mu + a, \tag{2b}$$

$$\text{and spin flip:} \quad a\mu(F) + a \to a\mu(F') + a. \tag{2c}$$

The application of the nuclear cross sections to a description of experiments performed in molecular targets gives very unsatisfactory results. A characteristic kinetic energy of muonic atoms in typical gaseous targets is lower than a few eV [16]. Therefore, it is necessary to take into account effects of molecular binding and electron screening.

Since a muonic hydrogen atom is a small neutral system, the methods developed for the description of neutron scattering in matter can be adapted, to a certain extent, for the muonic atom case. Molecular effects in low-energy neutron scattering from nuclei bound in chemical compounds are estimated using the Fermi pseudopotential [17–19]. Such a pseudopotential is proportional to the constant scattering length. The Fermi method was used for decades for the calculation of low-energy neutron cross sections (see, e.g., Ref. [20] and references therein). In particular, a quantum-mechanical treatment of slow neutron scattering from molecular hydrogen and deuterium was presented by Young and Koppel [21].

A method of calculating binding effects in the molecular processes (1), based on the Fermi approach, was derived in Refs. [22,23]. In particular, specific spin-dependent pseudopotentials were introduced for a description of a muonic atom interaction with a single nucleus. However, this method has a limited applicability since the nuclear processes (2) involve several partial scattering waves [5,8] even at low ($\sim$1 eV) energies, in contrast to low-energy neutron scattering. Moreover, muonic atom scattering often changes strongly (e.g., $p\mu$+p and $t\mu$+t) with energy in the intervals comparable with the rotational thresholds of hydrogenic molecules. A solution to this problem is to base a calculation of the molecular cross sections on the full nuclear scattering amplitudes, which include all the angular and energy dependence. The effective radius of interaction between a muonic

---

[*] Electronic address: andrzej.adamczak@ifj.edu.pl

atom and a nucleus is much smaller than the internuclear distance in a hydrogen molecule [1]. Therefore, the amplitude for scattering from two bound nuclei can be well approximated by a sum of the two corresponding amplitudes for scattering from isolated nuclei. In such an approach, it is necessary to take into account the internal motion of the nuclei inside a target molecule. This motion can be neglected for a molecule consisting of heavy nuclei. However, we are dealing with the lightest molecules and, therefore, the kinetic energy of nuclear motion due to zero-point vibration is on the order of 0.1 eV.

In Sec. II, the amplitudes for the molecular processes (1) are expressed in terms of the amplitudes of the three-body reactions (2). The derived formulas depend on the momenta of internal motion of the nuclei in a target molecule. The differential cross sections for scattering from molecules are obtained in Sec. III, using a harmonic model of molecular vibrations. Also, electron-screening corrections to the cross sections are given in this section. Some typical examples of the computed differential cross sections are shown in Sec. IV.

II. AMPLITUDES FOR SCATTERING FROM MOLECULES

Let us consider $a\mu$ scattering from a molecule BC consisting of hydrogen-isotope nuclei b and c and two electrons. First, we assume that the nuclei b and c are different from the nucleus a, so that the scattering is spin independent [1,2]. Also, electron-screening effects are neglected in this section. The scattering lengths of the processes $a\mu+b$ (c) [5,8] are much smaller than the molecular diameter $R_0 \approx 300 a_\mu$ (a_μ denotes the Bohr radius of the $a\mu$ atom). The interaction of a muonic hydrogen atom with nucleus b (or c) is important at distances $\ll R_0$ [1]. Hence, it is assumed that $a\mu$ interacts with a single nucleus during the collision with the molecule. We also assume that the molecular bond is unperturbed at the moment of collision. Therefore, $a\mu$ collision with $b(c)$ is treated here as if this nucleus were free, except for its momentum distribution due to the molecular binding [24]. This means that the amplitude for $a\mu$ scattering from a bound nucleus is the same as that for an identical free nucleus, provided the momentum of the relative motion is not changed.

At large distances between $a\mu$ and BC, the initial ψ_0 and final ψ_n coordinate wave functions of the system are as follows:

$$\psi_0(\mathbf{r},\mathbf{r}_\mu,\mathbf{R}) = \phi_i(\mathbf{r}_\mu)\Phi_0(\mathbf{R})\exp(i\mathbf{k}_0\cdot\mathbf{r}),$$

$$\psi_n(\mathbf{r},\mathbf{r}_\mu,\mathbf{R}) = \phi_f(\mathbf{r}_\mu)\Phi_n(\mathbf{R})\exp(i\mathbf{k}_n\cdot\mathbf{r}), \tag{3}$$

where $\mathbf{k}_0$ and $\mathbf{k}_n$ are the initial and final momenta of $a\mu$; Φ_0 and Φ_n are the wave functions of the initial and final rotational-vibrational states of the molecule BC. The corresponding wave functions of the $1S$ muonic atom are denoted by ϕ_i and ϕ_f, where the indices i and f refer to the processes (2) with the nuclear scattering amplitudes f_{if} [3–8]. In Fig. 1, the relative coordinates used for providing a description of the system are shown. The vector $\mathbf{R}$ connects nucleus b with nucleus c; $\mathbf{r}$ denotes the $a\mu$ position with respect to the center of mass (c.m.) of BC; $\mathbf{r}_\mu$ is the $a\mu$ internal vector. The vector $\mathbf{r}_b$ stands for the $a\mu$ position relative to nucleus b.

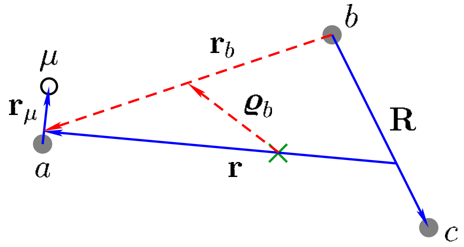

FIG. 1. (Color online) Relative coordinates used for the description of muonic atom $a\mu$ scattering from a molecule BC. The cross denotes the position of the center of mass of this system.

It is convenient to express the amplitude for $a\mu$ scattering from BC in terms of the momenta $\mathbf{k}_0$ and $\mathbf{k}_n$ in the center-of-mass system (c.m.s.) for $a\mu+BC$. On the other hand, the calculated amplitudes for $a\mu$ scattering from nuclei are functions of the initial $\mathbf{p}_b$ and final $\mathbf{p}'_b$ momenta in the c.m.s. of $a\mu+b$. Therefore, further evaluation of the molecular amplitudes involves the investigation of a transition between the nuclear and molecular momenta. First, we assume that both the nuclear and molecular scattering can be described in the Born approximation. The amplitude for $a\mu$ scattering from b bound in BC is thus given by the following formula (in muonic atomic units $e=\hbar=\mu_{a\mu}=1$):

$$\mathcal{F}^{(b)}_{0n}(\mathbf{k}_0,\mathbf{k}_n) = -\frac{\mathcal{M}}{2\pi}\int d^3r\, d^3r_\mu d^3R \exp[i(\mathbf{k}_0-\mathbf{k}_n)\cdot\mathbf{r}] \times \Phi^*_n(\mathbf{R})\phi^*_f(\mathbf{r}_\mu)V^{(b)}(\mathbf{r}_b,\mathbf{r}_\mu)\phi_i(\mathbf{r}_\mu)\Phi_0(\mathbf{R}), \tag{4}$$

where $\mathcal{M}$ is the reduced mass of the $a\mu+BC$ system (the masses of the electrons are neglected) and $\mu_{a\mu}$ is the reduced mass of the $a\mu$ atom,

$$\mathcal{M}^{-1} = M^{-1}_{a\mu} + M^{-1}_{\text{mol}}, \quad \mu^{-1}_{a\mu} = M^{-1}_a + m^{-1}_\mu,$$

$$M_{a\mu} = M_a + m_\mu, \quad M_{\text{mol}} = M_b + M_c.$$

The potential of $a\mu$ interaction with a free nucleus b is denoted by $V^{(b)}$. Using the relation

$$\mathbf{r}_b = \mathbf{r} + \beta_b\mathbf{R}, \quad \beta_b = M_c/(M_b+M_c), \tag{5}$$

in Eq. (4) leads to the following factorization:

$$\mathcal{F}^{(b)}_{0n} = -\frac{\mathcal{M}}{2\pi}\int d^3r_b \exp[i(\mathbf{k}_0-\mathbf{k}_n)\cdot\mathbf{r}_b]V^{(b)}_{if}(\mathbf{r}_b) \times \int d^3R \exp[i\beta_b(\mathbf{k}_0-\mathbf{k}_n)\cdot\mathbf{R}]\Phi^*_n(\mathbf{R})\Phi_0(\mathbf{R}), \tag{6}$$

in which $V^{(b)}_{if}$ denotes the nuclear matrix element

$$V^{(b)}_{if}(\mathbf{r}_b) \equiv \int d^3r_\mu \phi^*_f(\mathbf{r}_\mu)V^{(b)}(\mathbf{r}_b,\mathbf{r}_\mu)\phi_i(\mathbf{r}_\mu). \tag{7}$$

The first integral in Eq. (6) is the Born amplitude for $a\mu$ scattering from a free nucleus b times the factor $\mathcal{M}/\mu_b$, where μ_b stands for the reduced mass of the system $a\mu+b$:

$$\mu_b^{-1} = (m_\mu + M_a)^{-1} + M_b^{-1}.$$

The second integral in Eq. (6) is a form factor describing the binding of b in BC.

In order to investigate the dependence of the molecular amplitude $\mathcal{F}_{0n}^{(b)}$ on the internal motion of b inside the molecule, a momentum representation of the wave function Φ_n is introduced,

$$\Phi_n(\mathbf{R}) \equiv \frac{1}{(2\pi)^{3/2}} \int d^3\kappa_n \exp(i\beta_b \boldsymbol{\kappa}_n \cdot \mathbf{R}) g_n^{(b)}(\boldsymbol{\kappa}_n),$$

$$g_n^{(b)}(\boldsymbol{\kappa}_n) \equiv \frac{\beta_b^3}{(2\pi)^{3/2}} \int d^3R \exp(-i\beta_b \boldsymbol{\kappa}_n \cdot \mathbf{R}) \Phi_n(\mathbf{R}). \qquad (8)$$

The vector $\boldsymbol{\kappa}_n$ is the momentum of the internal nuclear motion in the final rotational-vibrational state n. The analogous equations can be written down for the initial molecular state Φ_0 with the internal nuclear momentum $\boldsymbol{\kappa}_0$. Upon substituting Eq. (8) into Eq. (4) one obtains

$$\mathcal{F}_{0n}^{(b)} = -\frac{\mathcal{M}}{(2\pi)^4} \int d^3r\, d^3R\, d^3\kappa_n d^3\kappa_0 \exp[i(\mathbf{k}_0 - \mathbf{k}_n)\cdot \mathbf{r}]$$
$$\times \exp[i\beta_b(\boldsymbol{\kappa}_0 - \boldsymbol{\kappa}_n)\cdot \mathbf{R}] V_{if}^{(b)}(\mathbf{r}_b) g_n^{(b)*}(\boldsymbol{\kappa}_n) g_0^{(b)}(\boldsymbol{\kappa}_0). \qquad (9)$$

Then, using new variables $\mathbf{r}_b$ and $\boldsymbol{\varrho}_b$

$$\mathbf{r} = \frac{\mu_b}{\mathcal{M}}\mathbf{r}_b + \beta_b \frac{M_{abc}}{M_c}\boldsymbol{\varrho}_b, \quad \mathbf{R} = \frac{M_a}{M_{ab}}\mathbf{r}_b - \frac{M_{abc}}{M_c}\boldsymbol{\varrho}_b,$$

$$M_{abc} = M_a + M_b + M_c, \quad M_{ab} = M_a + M_b, \qquad (10)$$

in Eq. (9) and performing integration over the vector $\mathbf{x} = (\beta_b M_{abc}/M_c)\boldsymbol{\varrho}_b$, one has

$$\mathcal{F}_{0n}^{(b)} = -\frac{\mathcal{M}}{2\pi\beta_b^3} \int d^3\kappa_n d^3\kappa_0 \int d^3r_b$$
$$\times \exp\left[-i\left(\frac{\mu_b}{\mathcal{M}}\mathbf{k}_n + \beta_b \frac{\mu_b}{M_b}\boldsymbol{\kappa}_n\right)\cdot \mathbf{r}_b\right]$$
$$\times V_{if}^{(b)}(\mathbf{r}_b) \exp\left[i\left(\frac{\mu_b}{\mathcal{M}}\mathbf{k}_0 + \beta_b \frac{\mu_b}{M_b}\boldsymbol{\kappa}_0\right)\cdot \mathbf{r}_b\right]$$
$$\times \delta(\mathbf{k}_0 - \mathbf{k}_n - \boldsymbol{\kappa}_0 + \boldsymbol{\kappa}_n) g_n^{(b)*}(\boldsymbol{\kappa}_n) g_0^{(b)}(\boldsymbol{\kappa}_0). \qquad (11)$$

The integral over $\mathbf{r}_b$ times $-\mu_b/2\pi$ is the Born amplitude $f_{if}^{(b)}$ for $a\mu$ scattering on a free nucleus b, expressed by the momenta $\mathbf{k}_n$, $\boldsymbol{\kappa}_n$, $\mathbf{k}_0$, and $\boldsymbol{\kappa}_0$. Thus, Eq. (11) can be written down in the following form:

$$\mathcal{F}_{0n}^{(b)} = \frac{1}{\beta_b^3}\frac{\mathcal{M}}{\mu_b} \int d^3\kappa_n d^3\kappa_0 f_{if}^{(b)}$$
$$\times \left(\frac{\mu_b}{\mathcal{M}}\mathbf{k}_0 + \beta_b \frac{\mu_b}{M_b}\boldsymbol{\kappa}_0, \frac{\mu_b}{\mathcal{M}}\mathbf{k}_n + \beta_b \frac{\mu_b}{M_b}\boldsymbol{\kappa}_n\right)$$
$$\times \delta(\mathbf{k}_0 - \mathbf{k}_n - \boldsymbol{\kappa}_0 + \boldsymbol{\kappa}_n) g_n^{(b)*}(\boldsymbol{\kappa}_n) g_0^{(b)}(\boldsymbol{\kappa}_0), \qquad (12)$$

where subscripts i and f label the kind of nuclear process (2). Now, we make the basic assumption that Eq. (12) is satisfied by the *exact* nuclear amplitudes $f_{if}^{(b)}$. The integration over $\boldsymbol{\kappa}_n$ is performed readily using the conservation of the total momentum, which gives

$$\mathcal{F}_{0n}^{(b)}(\mathbf{k}_0, \mathbf{q}) = \frac{1}{\beta_b^3}\frac{\mathcal{M}}{\mu_b} \int d^3\kappa_0 f_{if}^{(b)}(\mathbf{p}_b, \mathbf{p}_b + \mathbf{q})$$
$$\times g_n^{(b)*}(\boldsymbol{\kappa}_0 + \mathbf{q}) g_0^{(b)}(\boldsymbol{\kappa}_0), \qquad (13)$$

$$\mathbf{p}_b \equiv \frac{\mu_b}{\mathcal{M}}\mathbf{k}_0 + \beta_b \frac{\mu_b}{M_b}\boldsymbol{\kappa}_0, \quad \mathbf{p}_b' \equiv \mathbf{p}_b + \mathbf{q}. \qquad (14)$$

The vector $\mathbf{q}$ denotes the momentum transfer

$$\mathbf{q} = \mathbf{k}_n - \mathbf{k}_0 = \mathbf{p}_b' - \mathbf{p}_b. \qquad (15)$$

Thus, the molecular amplitude $\mathcal{F}_{0n}^{(b)}$ for scattering with a fixed momentum transfer $\mathbf{q}$ is determined by the free nuclear amplitude $f_{if}^{(b)}$ with the same momentum transfer. However, the initial momentum $\mathbf{p}_b$ in the $a\mu+b$ c.m.s. is different from the initial momentum $\mathbf{k}_0$ in the molecular c.m.s. According to Eq. (14), the vector $\mathbf{p}_b$ depends also on the internal motion of b. This gives the following $a\mu$ kinetic energy in the $a\mu+b$ c.m.s.:

$$\varepsilon_b = \frac{\mu_b}{\mathcal{M}}\varepsilon + \beta_b^2 \frac{\mu_b}{\mu_{bc}}\varepsilon_{bc} + 2\beta_b \frac{\mu_b}{\sqrt{\mu_{bc}\mathcal{M}}}\sqrt{\varepsilon\varepsilon_{bc}}\cos\theta, \qquad (16)$$

where θ is the angle between the vectors $\mathbf{k}_0$ and $\boldsymbol{\kappa}_0$. The muonic atom kinetic energies in the nuclear (ε_b) and molecular (ε) c.m.s. are

$$\varepsilon_b = \frac{p_b^2}{2\mu_b}, \quad \varepsilon = \frac{k_0^2}{2\mathcal{M}}. \qquad (17)$$

The internal kinetic energy ε_{bc} of the molecule BC is

$$\varepsilon_{bc} = \frac{\kappa_0^2}{2\mu_{bc}}, \quad \mu_{bc}^{-1} = M_b^{-1} + M_c^{-1}. \qquad (18)$$

At $\varepsilon \to 0$, the collision energy ε_b in the $a\mu+b$ system is determined solely by ε_{bc}. This energy never vanishes because of the zero-point vibration of the molecule. In particular, for the lightest H_2 molecule, the second term of Eq. (16) is on the order of 0.01 eV. This energy is inaccessible, but it affects the molecular scattering amplitude (13). For a fixed ε, the spectrum of ε_b is quite wide. Its width is determined by the term $\sqrt{\varepsilon\varepsilon_{bc}}$, which depends on the hydrogenic-molecule vibrational quantum ($\approx 0.3-0.5$ eV). Therefore, at a given ε, the molecular amplitude (13) contains contributions from the nuclear amplitude f_{if} taken at different energies. This effect should be taken into account when f_{if} changes significantly within the spectrum (16) of ε_b, which often occurs in muonic atom scattering.

If $k_0 \gg \kappa_0$ and $k_n \gg \kappa_n$, the dependence of $\mathbf{p}_b$ on $\boldsymbol{\kappa}_0$ in Eq. (14) can be neglected. As a result, we get

$$\mathbf{p}_b \approx \frac{\mu_b}{\mathcal{M}}\mathbf{k}_0 \qquad (19)$$

and Eq. (13) is then factorized as follows:

$$\mathcal{F}_{0n}^{(b)} = \frac{1}{\beta_b^3}\frac{\mathcal{M}}{\mu_b} f_{if}^{(b)}(\mathbf{p}_b,\mathbf{p}_b+\mathbf{q}) \int d^3\kappa_0\, g_n^{(b)*}(\boldsymbol{\kappa}_0+\mathbf{q})\, g_0^{(b)}(\boldsymbol{\kappa}_0). \tag{20}$$

This formula can also be used when $f_{if}^{(b)}$ weakly depends on the variation of p_b due to the characteristic spectrum of $\boldsymbol{\kappa}_0$. After the substitution of the Fourier transforms (8) into Eq. (20) and integration over $\boldsymbol{\kappa}_0$, we obtain

$$\mathcal{F}_{0n}^{(b)} = \frac{\mathcal{M}}{\mu_b} f_{if}^{(b)}\left(\frac{\mu_b}{\mathcal{M}}\mathbf{k}_0, \frac{\mu_b}{\mathcal{M}}\mathbf{k}_0+\mathbf{q}\right) \times \int d^3R\, \Phi_n^*(\mathbf{R}) \exp(i\beta_b \mathbf{q}\cdot\mathbf{R}) \Phi_0(\mathbf{R}). \tag{21}$$

The molecular scattering amplitudes (13) and (21) naturally take into account the dependence of the nuclear amplitude f_{if} on the $a\mu$ energy and scattering angle ϑ. At low collision energies, the amplitudes f_{if} are well approximated by the corresponding constant scattering lengths λ_{if}^0. As a result, Eq. (21) is simplified:

$$\mathcal{F}_{0n}^{(b)}(\mathbf{q}) \approx -\frac{\mathcal{M}}{\mu_b}\lambda_{if}^{(b)0} \int d^3R\, \Phi_n^*(\mathbf{R}) \exp(i\beta_b \mathbf{q}\cdot\mathbf{R}) \Phi_0(\mathbf{R}),$$

$$\mathcal{F}_{0n}^{(b)}(\mathbf{q}) \xrightarrow[q\to 0]{} -\frac{\mathcal{M}}{\mu_b}\lambda_{if}^{(b)0}. \tag{22}$$

This equation can be formally obtained in the first Born approximation, using the pseudopotential

$$V_{if}^{(b)}(\mathbf{r}_b) = \frac{2\pi}{\mu_b}\lambda_{if}^{(b)0}\delta(\mathbf{r}_b) = \frac{2\pi}{\mu_b}\lambda_{if}^{(b)0}\delta(\mathbf{r}+\beta_b\mathbf{R}) \tag{23}$$

in Eq. (4). Such a potential for a constant scattering length was first introduced by Fermi [17] and more rigorously derived by Breit [18] and then by Lippmann and Schwinger [19].

In the case of a general spherical potential with a finite range, it is possible to generalize the Fermi pseudopotential by the introduction of partial pseudopotentials corresponding to subsequent scattering waves [25,26]. However, the calculations of the cross sections for muonic atom scattering on molecules, presented in this paper, are directly based on a knowledge of the amplitudes for nuclear scattering. Therefore, a formulation of a generalized pseudopotential, in this case, is superfluous. Let us only note that the correct nuclear partial amplitudes can be formally obtained by the substitution of the following pseudopotentials:

$$V_{if}^{(b)J}(\mathbf{r}_b) = \frac{2\pi}{\mu_b}(2J+1)\lambda_{if}^{(b)J}(p_b)\delta(\mathbf{r}_b)\mathrm{P}_J(\cos\vartheta_b) \tag{24}$$

into Eq. (4). The energy-dependent nuclear scattering length $\lambda_{if}^{(b)J}$ is defined as follows:

$$f_{if}^{(b)J} = -(2J+1)\lambda_{if}^{(b)J}\mathrm{P}_J(\cos\vartheta_b), \tag{25}$$

where $f_{if}^{(b)J}$ are the partial nuclear amplitudes for $a\mu+b$ scattering [3–8] and J is the angular momentum of the $a\mu+b$ system. The angle between the vectors $\mathbf{p}_b$ and $\mathbf{p}_b'$ is denoted here by ϑ_b. The function P_J is the Jth Legendre polynomial.

The problem of the angular and energy dependence of the nuclear scattering $t\mu+d$ in the $t\mu+\mathrm{D}_2$ process was alternatively solved in Ref. [27] by the introduction of the effective polarization potential ($\sim r^{-4}$). However, the magnitude of such a potential for the $t\mu$-d interaction was determined separately for every given collision energy. Thus, such an approach is more complicated than the direct use of the computed nuclear-scattering amplitudes and neglects a wide distribution of the deuteron kinetic energies in the D_2 molecule.

When the internal motion of the nuclei inside the target molecule cannot be neglected, the molecular amplitude is given by Eq. (13). However, in a general case, the numerical evaluation of the integrals over $\boldsymbol{\kappa}_0$ is difficult. The role of the internal motion is most important if the condition $q \ll \kappa_0$ is satisfied, which implies that the internal state of the molecule is not changed ($g_n^{(b)}=g_0^{(b)}$). In this case, Eq. (13) is approximated as follows:

$$\mathcal{F}_{00}^{(b)}(k_0) \approx \frac{\mathcal{M}}{\mu_b}\overline{f_{if}^{(b)}}(k_0),$$

$$\overline{f_{if}^{(b)}}(k_0) \equiv \int d^3\kappa_0 f_{if}^{(b)}(\mathbf{p}_b,\mathbf{p}_b')\mathcal{P}_0^{(b)}(\boldsymbol{\kappa}_0), \tag{26}$$

with $\mathcal{P}_0^{(b)}(\boldsymbol{\kappa}_0)$ being the distribution of the momentum of nucleus b in the molecule:

$$\mathcal{P}_0^{(b)}(\boldsymbol{\kappa}_0) \equiv \beta_b^{-3}|g_0^{(b)}(\boldsymbol{\kappa}_0)|^2. \tag{27}$$

For elastic scattering at $k_0 \to 0$, when one expects that the internal-motion effect is the strongest, the molecular scattering amplitude is

$$\mathcal{F}_{00}^{(b)} \approx -\frac{\mathcal{M}}{\mu_b}\overline{\lambda_{if}^{(b)0}}, \tag{28}$$

where the overbar denotes averaging over $\boldsymbol{\kappa}_0$. Equations (26) and (28) suggest a reasonable approximation of formula (13) for finite k_0. When the exact nuclear amplitude $f_{if}^{(b)}$ is replaced by the averaged function

$$\overline{f_{if}^{(b)}}(\mathbf{k}_0,\mathbf{q}) \equiv -\sum_J (2J+1)\overline{\lambda_{if}^{(b)J}}(k_0)\mathrm{P}_J(\cos\vartheta_b),$$

$$\overline{\lambda_{if}^{(b)J}}(k_0) \equiv \int d^3\kappa_0 \lambda_{if}^{(b)J}(p_b)\mathcal{P}_0^{(b)}(\boldsymbol{\kappa}_0), \tag{29}$$

Eq. (13) is factorized. This leads, finally, to an equation similar to Eq. (21), with $f_{if}^{(b)}$ replaced by the mean amplitude $\overline{f_{if}^{(b)}}$. This approximation gives the limit (28) at $k_0 \to 0$. On the other hand, this approximation coincides with the asymptotic amplitude (21) at $k_0 \gg \kappa_0$. The dependence of ϑ_b on $\boldsymbol{\kappa}_0$ is neglected here since the higher partial waves ($J>0$) in the nuclear scattering are important only at $k_0 \gg \kappa_0$.

III. MOLECULAR DIFFERENTIAL CROSS SECTIONS

A. Spin-independent scattering

In the presented approach, the total amplitude $\mathcal{F}_{0n}$ for $a\mu$ scattering on a molecule BC is equal to the sum of the amplitudes for scattering on the bound nuclei b and c,

$$\mathcal{F}_{0n}(\mathbf{k}_0,\mathbf{q}) = \mathcal{F}^{(b)}_{0n}(\mathbf{k}_0,\mathbf{q}) + \mathcal{F}^{(c)}_{0n}(\mathbf{k}_0,\mathbf{q}), \tag{30}$$

where $\mathcal{F}^{(b)}_{0n}$ is given by Eq. (21), and the derivation of $\mathcal{F}^{(c)}_{0n}$ is analogous. Let us first consider the spin-independent case $a \neq b$, c. Assuming that vibrations of the molecule are harmonic and that there is no coupling between the vibrational and rotational degrees of freedom, the molecular wave function $\Phi_n(\mathbf{R})$ takes the form

$$\Phi_n(\mathbf{R}) = \frac{u_\nu(R)}{R}\mathrm{Y}_{KM_K}(\hat{R}), \quad \hat{R} \equiv \frac{\mathbf{R}}{R}, \tag{31}$$

where the quantum numbers K and M_K label the rotational state of BC. The radial wave function u_ν corresponding to the vibrational quantum number ν is

$$u_\nu(R) = \mathcal{N}_\nu \mathrm{H}_\nu(\alpha(R-R_0))\exp\left[-\tfrac{1}{2}\alpha^2(R-R_0)^2\right],$$

$$\mathcal{N}_\nu = \sqrt{\frac{\alpha}{\sqrt{\pi}2^\nu \nu!}}, \quad \alpha = \sqrt{\mu_{bc}\,\omega_0}, \tag{32}$$

where H_ν denotes the νth Hermite polynomial. The rotational E_K and vibrational E_ν energy levels are given as

$$E_K = B_{\mathrm{rot}}K(K+1), \quad E_\nu = \left(\nu + \tfrac{1}{2}\right)\omega_0. \tag{33}$$

At the temperatures usually applicable to experiments, hydrogenic molecules are initially in the ground vibrational state $\nu=0$.

Inserting the expansion of the free-wave function (in terms of the spherical Bessel functions j_l and the spherical harmonics Y_{lm}) into Eq. (21), one obtains for the bound nucleus b

$$\mathcal{F}^{(b)}_{0n} = 4\pi\frac{\mathcal{M}}{\mu_b}f^{(b)}_{if}\sum_{l,m} i^l \mathcal{D}_{\nu l}(\beta_b q)\mathrm{Y}^*_{lm}(\hat{q}) \times \int d\Omega_R \mathrm{Y}^*_{K'M'_K}(\hat{R})\mathrm{Y}_{lm}(\hat{R})\mathrm{Y}_{KM_K}(\hat{R}). \tag{34}$$

The real function $\mathcal{D}_{\nu l}(\beta_b q)$ is a result of the integration over R,

$$\mathcal{D}_{\nu l}(\beta_b q) \equiv \int_0^\infty dR\, u_\nu(R)\mathrm{j}_l(\beta_b q R)u_0(R),$$

$$\mathcal{D}_{\nu l}(\beta_b q) \xrightarrow[q\to 0]{} \begin{cases} 1 & \text{if } \nu=0 \text{ and } l=0, \\ 0 & \text{otherwise}. \end{cases} \tag{35}$$

The initial state of the molecule is denoted here by the set of rotational and vibrational quantum numbers $0=(K,M_K,\nu=0)$. The final state is labeled by $n=(K',M'_K,\nu)$. The indices i and f in the nuclear amplitude $f^{(b)}_{if}$ refer to the initial and final states (spin or isotopic) of the scattered muonic atom. Integration of the three spherical harmonics in Eq. (34) over the solid angle Ω_R leads to the following result:

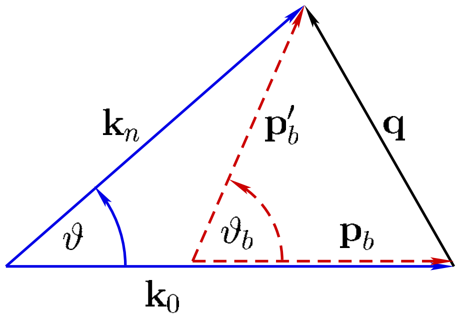

FIG. 2. (Color online) Relations between the initial and final momenta and between the scattering angles ϑ_b and ϑ in the nuclear and molecular c.m.s. (for $k_0 \gg \kappa_0$).

$$\mathcal{F}^{(b)}_{0n} = [4\pi(2K'+1)(2K+1)]^{1/2}(-1)^{M'_K}i^{K-K'} \times \frac{\mathcal{M}}{\mu_b}f^{(b)}_{if}\sum_{l,m}(2l+1)^{1/2}\mathcal{D}_{\nu l}(\beta_b q)\mathrm{Y}^*_{lm}(\hat{q}) \times \begin{pmatrix} K' & l & K \\ 0 & 0 & 0 \end{pmatrix}\begin{pmatrix} K' & l & K \\ -M'_K & m & M_K \end{pmatrix}, \tag{36}$$

expressed by the Wigner $3j$ symbols.

The molecular differential cross section, averaged over the projection M_K of the initial angular momentum and summed over the projection M'_K of the final angular momentum, is equal to

$$\frac{d\sigma_{0n}}{d\Omega} = \frac{k_n}{k_0}\frac{1}{2K+1}\sum_{M_K,M'_K}|\mathcal{F}^{\mathrm{mol}}_{0n}|^2. \tag{37}$$

The solid angle $\Omega(\vartheta,\varphi)$ is connected with the direction of the vector $\mathbf{k}_n$ with respect to the initial $a\mu$ momentum $\mathbf{k}_0$ (see Fig. 2). Substitution of Eq. (36) and the analogous formula for the nucleus c into Eqs. (30) and (37) gives the following cross section:

$$\frac{d\sigma_{0n}}{d\Omega} = \frac{k_n}{k_0}\sum_l \mathcal{W}_{K'lK}\left[\left(\frac{\mathcal{M}}{\mu_b}\right)^2|f^{(b)}_{if}|^2\mathcal{D}^2_{\nu l}(\beta_b q) + (-1)^l 2\frac{\mathcal{M}^2}{\mu_b\mu_c}\mathrm{Re}(f^{(b)*}_{if}f^{(c)}_{if})\mathcal{D}_{\nu l}(\beta_b q)\mathcal{D}_{\nu l}(\beta_c q) + \left(\frac{\mathcal{M}}{\mu_c}\right)^2|f^{(c)}_{if}|^2\mathcal{D}^2_{\nu l}(\beta_c q)\right], \tag{38}$$

where the angular-momentum factor $\mathcal{W}_{K'lK}$ is defined as

$$\mathcal{W}_{K'lK} \equiv (2K'+1)(2l+1)\begin{pmatrix} K' & l & K \\ 0 & 0 & 0 \end{pmatrix}^2, \quad \mathcal{W}_{K0K} = 1. \tag{39}$$

The reduced mass of the $a\mu + c$ system is

$$\mu_c^{-1} = (m_\mu + M_a)^{-1} + M_C^{-1}$$

and

$$\beta_c = 1 - \beta_b = M_b/(M_b + M_c).$$

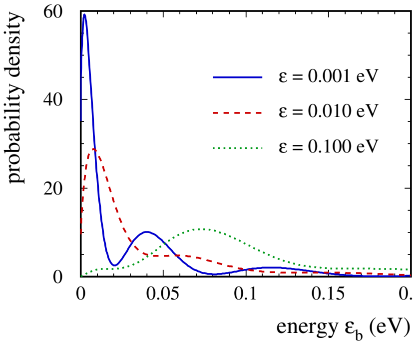

FIG. 3. (Color online) Distribution of collision energy ε_b in the $p\mu+p$ c.m.s., for a fixed collision energy ε in the $p\mu+\mathrm{H}_2(K=0)$ c.m.s.

When BC is symmetric ($b=c$, $\mu_b=\mu_c=\mu$, $\beta_b=\beta_c=\beta=\frac{1}{2}$, and $f_{if}^{(b)}=f_{if}^{(c)}=f_{if}$), Eq. (38) takes the simpler form

$$\frac{d\sigma_{0n}}{d\Omega} = 2\left(\frac{\mathcal{M}}{\mu}\right)^2 |f_{if}|^2 \frac{k_n}{k_0}\sum_l [(-1)^l+1]\mathcal{W}_{K'lK}\mathcal{D}^2_{\nu l}(\beta q). \tag{40}$$

The molecular cross sections (38) and (40) directly include the dependence of the "bare" nuclear amplitudes f_{if} on the collision energy ε_b (ε_c) and on the scattering angle ϑ_b (ϑ_c). They are derived for high collision energies $k_0 \gg \kappa_0$. However, they can also be used at lower energies as a reasonable approximation if the nuclear amplitudes $f_{if}^{(b)}$ ($f_{if}^{(c)}$) are replaced by the amplitudes $\overline{f_{if}^{(b)}}$ ($\overline{f_{if}^{(c)}}$) averaged over $\mathcal{P}_0^{(b)}$ ($\mathcal{P}_0^{(c)}$). In the case of the wave function (31), the momentum distribution (27) for the ground vibrational state $\nu=0$ of the molecule BC has the form

$$\mathcal{P}_0^{(b)}(\boldsymbol{\kappa}_0) = 4\frac{\beta_b^3 R_0^2}{\alpha\sqrt{\pi}}\mathrm{j}_K^2(\beta_b\kappa_0 R_0)\exp\left(-\frac{\beta_b^2\kappa_0^2}{\alpha^2}\right)|\mathrm{Y}_{KM_K}(\hat{\kappa}_0)|^2, \tag{41}$$

in which $\hat{\kappa}_0=\boldsymbol{\kappa}_0/\kappa_0$. After averaging $\mathcal{P}_0^{(b)}$ over orientations of the molecule, one obtains

$$\mathcal{P}_0^{(b)}(\kappa_0) = \frac{\beta_b^3 R_0^2}{\alpha\pi^{3/2}}\mathrm{j}_K^2(\beta_b\kappa_0 R_0)\exp\left(-\frac{\beta_b^2\kappa_0^2}{\alpha^2}\right). \tag{42}$$

A distribution $\mathcal{P}_{0K}$ of the internal kinetic energy ε_{bc} of the target molecule can be derived similarly. For $\nu=0$, one has

$$\mathcal{P}_{0K}(\varepsilon_{bc})d\varepsilon_{bc} = \frac{2R_0^2\alpha^2}{\pi}\mathrm{j}_K^2(R_0\alpha\sqrt{\omega_{bc}})\exp(-\omega_{bc})\sqrt{\omega_{bc}}\,d\omega_{bc}, \tag{43}$$

where $\omega_{bc}=2\varepsilon_{bc}/\omega_0$. This distribution is widest for the lightest H_2 molecule. According to Eq. (16), this leads to a broad distribution of the collision energy ε_b in the nuclear c.m.s. for a fixed collision energy ε in the molecular c.m.s. In Figs. 3 and 4, the calculated ε_b spectrum for the ground-state H_2 molecule at several values of ε is presented. At the lowest energies, the shape of this spectrum is mainly determined by the motion of a bound proton. The mean value of ε_b equals 0.036 eV for $\varepsilon=0.001$ eV. For $\varepsilon=0.1$ eV, a single broad peak with a mean value of 0.11 eV is observed in the ε_b spectrum. Only at $\varepsilon \gtrsim 1$ eV does the average ε_b approach the asymptotic value of $(\mu_b/\mathcal{M})\varepsilon$ given by the first term of Eq. (16). However, the width of the ε_b distribution, determined by the last term of this equation, increases with rising ε. The ratio of this width to the mean value of ε_b decreases as $\varepsilon^{-1/2}$.

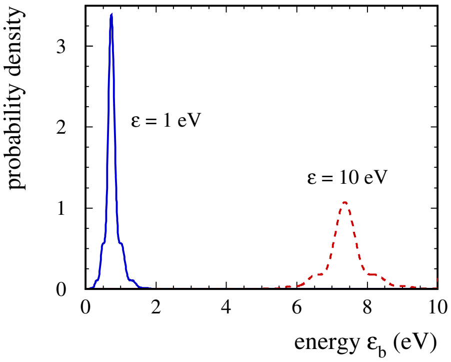

FIG. 4. (Color online) The same as in Fig. 3, for $\varepsilon=1$ and 10 eV.

B. Spin-dependent scattering

When at least one of the nuclei bound in BC (e.g., the nucleus b) is identical with the nucleus a, it is necessary to consider spin-dependent reactions (2a) and (2c). Let us introduce the following notation:

$$\begin{gathered}\mathcal{J} \equiv \mathbf{s}_\mu + \mathbf{s}_a + \mathbf{s}_b + \mathbf{s}_c,\\ \mathbf{F} \equiv \mathbf{s}_\mu + \mathbf{s}_a, \quad \mathbf{I} \equiv \mathbf{s}_b + \mathbf{s}_c,\\ \mathbf{S}_b \equiv \mathbf{F} + \mathbf{s}_b, \quad \mathbf{S}_c \equiv \mathbf{F} + \mathbf{s}_c,\\ \mathcal{J} = \mathbf{F} + \mathbf{I} = \mathbf{S}_b + \mathbf{s}_c = \mathbf{s}_b + \mathbf{S}_c,\end{gathered} \tag{44}$$

where $\mathbf{s}_\mu$, $\mathbf{s}_a$, $\mathbf{s}_b$, and $\mathbf{s}_c$ are the spins of the muon and of the nuclei a, b, and c, respectively. Thus, $\mathcal{J}$ is the total spin of $a\mu+BC$ system and $\mathbf{I}$ is the total nuclear spin of the molecule. It is assumed that $\mathcal{J}$ is conserved in the scattering since the spin-orbit interaction is very weak. Also, it is assumed that the spin $\mathbf{S}_b$ ($\mathbf{S}_c$) is conserved in local collisions of $a\mu$ with the nucleus b (c) bound in BC.

If the isotope c is different from a and b, the molecule BC is asymmetric and its parity is not definite. Thus, the directions of the nuclear spins $\mathbf{s}_b$ and $\mathbf{s}_c$ are independent of each other, and a unique spin $\mathbf{S}_b$ of the subsystem $a\mu+b$ is assigned to the initial ξ_i and final ξ_f spin states of the system $a\mu+BC$ (with fixed values of F and F'). These states can be written down as follows:

$$\begin{gathered}\xi_i(\mathbf{S}_b,\mathbf{s}_c;F) = \xi_{a\mu-b}(\mathbf{S}_b;F)\xi_c(\mathbf{s}_c),\\ \xi_f(\mathbf{S}_b,\mathbf{s}_c;F') = \xi_{a\mu-b}(\mathbf{S}_b;F')\xi_c(\mathbf{s}_c),\end{gathered} \tag{45}$$

where $\xi_{a\mu-b}$ and ξ_c are the eigenfunctions of the conserved spins $\mathbf{S}_b$ and $\mathbf{s}_c$, respectively. In this case, the total wave functions take the form

$$\psi_0 = \phi_i(\mathbf{r}_\mu)\Phi_0(\mathbf{R})\exp(i\mathbf{k}_0\cdot\mathbf{r})\xi_i(\mathbf{S}_b,\mathbf{s}_c;F),$$

$$\psi_n = \phi_f(\mathbf{r}_\mu)\Phi_n(\mathbf{R})\exp(i\mathbf{k}_n\cdot\mathbf{r})\xi_f(\mathbf{S}_b,\mathbf{s}_c;F'), \qquad (46)$$

at large distances r. In order to obtain the correct molecular-scattering amplitudes, symmetrization of the functions ψ_0,ψ_n over the two identical particles a and b should be performed. As a result, we obtain the molecular amplitude $\mathcal{F}^{(b)}_{0n}$ which is expressed by Eq. (36) with $f^{(b)}_{if}$ replaced by the spin-dependent nuclear amplitude $f^{S_b}_{FF'}$ for the process (2a) or (2c). The calculated amplitudes $f^{S_b}_{FF'}$ are already symmetrized over the identical nuclei [3–6]. Similarly, the total molecular cross section $d\sigma^{S_b}_{0n}/d\Omega$ for $a=b\neq c$ is given by Eq. (38) with $f^{(b)}_{if}$ replaced by $f^{S_b}_{FF'}$. In the case of a spin-flip reaction, we substitute $f^{(c)}_{if}=0$ in Eq. (38), because this process is very weak when the isotope b is different from a [28]. The cross section $d\sigma^{S_b}_{0n}/d\Omega$ can be averaged over the projections of spin S_b, which gives the mean cross section $d\sigma_{0n}/d\Omega$.

When all the hydrogen isotopes are identical, the molecule BC is symmetric and its initial and final parities P_I and P'_I are definite. Therefore, the values I and I' of the molecular spin are definite. The total spin functions of $a\mu+BC$ are now eigenstates of $\boldsymbol{\mathcal{J}}$ with fixed values of F and I (or F' and I'). Thus, the total spin state is determined by four quantum numbers: the absolute value $\mathcal{J}$ of the total spin $\boldsymbol{\mathcal{J}}$, its projection $\mathcal{J}_z$, F, and I. The initial and final total wave functions of the system with $a=b=c$ are

$$\psi_0 = \phi_i(\mathbf{r}_\mu)\Phi_0(\mathbf{R})\exp(i\mathbf{k}_0\cdot\mathbf{r})\xi_i(\boldsymbol{\mathcal{J}};F,I),$$

$$\psi_n = \phi_f(\mathbf{r}_\mu)\Phi_n(\mathbf{R})\exp(i\mathbf{k}_n\cdot\mathbf{r})\xi_f(\boldsymbol{\mathcal{J}};F',I'), \qquad (47)$$

with the following condition to be satisfied:

$$\mathbf{F}+\mathbf{I}=\mathbf{F}'+\mathbf{I}'=\boldsymbol{\mathcal{J}}. \qquad (48)$$

The functions ξ_i and ξ_f contain contributions from different states of the operator $\mathbf{S}_b$. They can be expanded as follows:

$$\xi_i(\boldsymbol{\mathcal{J}};F,I)=\sum_{\mathbf{S}_b} C_b(\mathbf{S}_b,\mathbf{s}_c;F,I)\xi_{a\mu-b}(\mathbf{S}_b)\xi_c(\mathbf{s}_c),$$

$$\xi_f(\boldsymbol{\mathcal{J}};F',I')=\sum_{\mathbf{S}_b} C'_b(\mathbf{S}_b,\mathbf{s}_c;F',I')\xi_{a\mu-b}(\mathbf{S}_b)\xi_c(\mathbf{s}_c), \qquad (49)$$

with $\mathbf{s}_c$ subject to the condition $\mathbf{S}_b+\mathbf{s}_c=\boldsymbol{\mathcal{J}}$. The factors $C_b(\mathbf{S}_b,\mathbf{s}_c;F,I)$ and $C'_b(\mathbf{S}_b,\mathbf{s}_c;F',I')$ are obtained by multiple use of the Clebsch-Gordan coefficients. The expansions of the total spin functions in terms of $\xi_{a\mu-b}(\mathbf{S}_b)$ are necessary since the presented method is based on knowledge of the three-body scattering amplitudes $f^{S_b}_{FF'}$ evaluated for fixed values of S_b.

After performing a symmetrization of the total potential $V^{(b)}+V^{(c)}$ and of the wave functions (47) over the three identical nuclei and proceeding as in Sec. II for the spinless case, one obtains

$$\mathcal{F}^{(b)}_{0n}=\frac{\mathcal{M}}{\mu}\sum_{\mathbf{S}_b} C_b(\mathbf{S}_b,\mathbf{s}_c;F,I)C'_b(\mathbf{S}_b,\mathbf{s}_c;F',I')f^{S_b}_{FF'}$$
$$\times\int d^3R\,\Phi^*_n(\mathbf{R})\exp(i\beta\mathbf{q}\cdot\mathbf{R})\Phi_0(\mathbf{R}). \qquad (50)$$

In the derivation of Eq. (50), it has been assumed that the three nuclei are never close together, i.e., the nucleus c is only a distant spectator when $a\mu$ collides with the nucleus b. As a result, the molecular amplitude (50) is expressed in terms of the three-body amplitudes $f^{S_b}_{FF'}$. By employing Eq. (50), the total molecular amplitude takes the form

$$\mathcal{F}_{0n}=\frac{\mathcal{M}}{\mu}\mathfrak{F}_{FF'}(K,K')\int d^3R\,\Phi^*_n(\mathbf{R})[\exp(i\beta\mathbf{q}\cdot\mathbf{R})$$
$$+P_IP_{I'}\exp(-i\beta\mathbf{q}\cdot\mathbf{R})\Phi_0(\mathbf{R})], \qquad (51)$$

where $\mathfrak{F}_{FF'}(I,I')$ is given as

$$\mathfrak{F}_{FF'}(I,I')\equiv\sum_{\mathbf{S}_b} C_b(\mathbf{S}_b,\mathbf{s}_c;F,I)C'_b(\mathbf{S}_b,\mathbf{s}_c;F',I')f^{S_b}_{FF'}. \qquad (52)$$

This result is independent of the choice of nucleus b because of the symmetry $b\leftrightarrow c$, $\mathbf{S}_b\leftrightarrow\mathbf{S}_c$, and $\mathbf{s}_c\leftrightarrow\mathbf{s}_b$. Using the expansion of the plane wave in terms of the spherical harmonics in Eq. (51) and taking into account that $[1+P_IP_{I'}(-1)^l]=2$ for every allowed rotational transition, we obtain

$$\frac{d\sigma_{0n}}{d\Omega}=4\left(\frac{\mathcal{M}}{\mu}\right)^2\overline{|\mathfrak{F}_{FF'}(K,K')|^2}\frac{k_n}{k_0}\sum_l \mathcal{W}_{K'lK}\mathcal{D}^2_{\nu l}(\beta q), \qquad (53)$$

in the case $a=b=c$. Since, in experiments, both the muonic atoms and the target molecules are not polarized, the cross section is averaged over $\mathcal{J}$ and I and summed over I' (for fixed K and K'), which is denoted by the horizontal bar over the squared amplitude $|\mathfrak{F}_{FF'}|^2$.

C. Electron-screening corrections to molecular cross sections

The differential molecular cross sections derived in the previous section include only the muonic-atom interaction with nuclei. It is necessary, however, to include the electron-screening effects in $a\mu$ scattering from molecules. At $\varepsilon\lesssim 1$ eV, the relative velocity of $a\mu$ and BC is smaller by several orders of magnitude than the muon velocity in $a\mu$ and is also smaller than the electron velocity in the molecule. Therefore, it is possible to introduce an effective electron-screening potential, which is obtained by averaging the Coulomb interaction between $a\mu$ and the electrons over the muon and the electron coordinates. The range of a dominant fraction of the $a\mu$-b potential is smaller than about $20a_\mu$ [1]. On the other hand, the $a\mu$ interaction with the electrons is important at distances on the order of the Bohr radius $a_e\approx 207a_\mu$ of the electronic hydrogen atom. Thus, $a\mu$ collision with an ordinary molecule can be described as scattering on the two potentials with very different ranges.

The effective screening potential V_{el} for $a\mu$ scattering from hydrogenic molecules has the following form [22,29]:

$$V_{\text{el}} = -\frac{\mathcal{C}\eta^3}{a_e^3(1+S_\eta^2)}\Bigg[\exp\left(-\frac{2\eta}{a_e}|\mathbf{r}+\beta_b\mathbf{R}|\right) + 2S_\eta\exp\left(-\frac{\eta}{a_e}(|\mathbf{r}+\beta_b\mathbf{R}|+|\mathbf{r}-\beta_c\mathbf{R}|)\right) + \exp\left(-\frac{2\eta}{a_e}|\mathbf{r}-\beta_c\mathbf{R}|\right)\Bigg], \tag{54}$$

in which

$$\mathcal{C} = 2\varkappa_\mu + 8.4\sqrt{m_e}, \quad \varkappa_\mu = (M_a - m_\mu)/(M_a + m_\mu),$$

and

$$S_\eta = \left(1 + w_\eta + \tfrac{1}{3}w_\eta^2\right)\exp(-w_\eta), \quad w_\eta = \frac{\eta R_0}{a_e}, \quad \eta = 1.2.$$

The electronic correction to the process (1a) is calculated using the first Born approximation. The total molecular amplitude $\mathcal{F}_{0n}^{\text{mol}}$ is now equal to the sum of the nuclear amplitudes and the screening amplitude $\mathcal{F}_{0n}^{\text{el}}$,

$$\mathcal{F}_{0n}^{\text{mol}}(\mathbf{k}_0,\mathbf{q}) = \mathcal{F}_{0n}^{(b)}(\mathbf{k}_0,\mathbf{q}) + \mathcal{F}_{0n}^{(c)}(\mathbf{k}_0,\mathbf{q}) + \mathcal{F}_{0n}^{\text{el}}(\mathbf{q}), \tag{55}$$

where

$$\mathcal{F}_{0n}^{\text{el}}(\mathbf{q}) = -\frac{\mathcal{M}}{2\pi}\int d^3r\, d^3R\, \exp(-i\mathbf{q}\cdot\mathbf{r}) \times \Phi_n^*(\mathbf{R})V_{\text{el}}(\mathbf{r},\mathbf{R})\Phi_0(\mathbf{R}). \tag{56}$$

The calculated amplitude $\mathcal{F}_{0n}^{\text{el}}$ falls rapidly when $qa_e \gtrsim 1$, which occurs even for the lowest rotational excitations of a hydrogenic molecule. Therefore, it is sufficient to take this amplitude into account only for the strictly elastic scattering. The isotopic exchange (2b) and the strong spin-flip (2c) reactions are due to the exchange of the muon between two nuclei taking part in direct collision. Therefore, $a\mu$ scattering from electrons cannot cause these reactions. The first nonvanishing screening corrections to the spin-flip or isotopic-exchange cross sections appear only in the distorted wave Born approximation.

A further evaluation of the screening corrections to the scattering amplitudes should be performed numerically. With regard to the elastic processes, these corrections are very significant. For example, at $\varepsilon \to 0$, the screening amplitude $\mathcal{F}_{0n}^{\text{el}}$ for $p\mu + \text{H}_2$ elastic scattering is comparable to the corresponding $p\mu + p$ scattering amplitude. In this limit, the relative screening corrections to the spin-flip or isotopic-exchange amplitudes are on the order of 10%. At $\varepsilon \gtrsim 1$ eV, screening effects practically vanish for all processes.

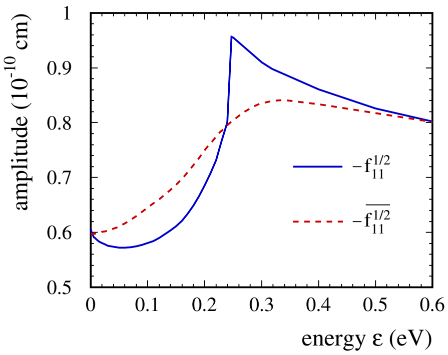

FIG. 5. (Color online) Amplitude $f_{11}^{1/2}$ and average amplitude $\overline{f_{11}^{1/2}}$ for $p\mu(F{=}0)+p$ scattering vs collision energy ε in the molecular c.m.s.

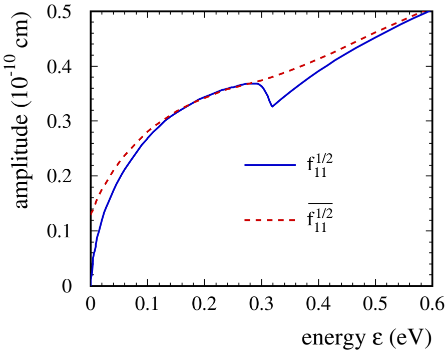

FIG. 6. (Color online) The same as in Fig. 5, for $t\mu(F{=}0)+t$ scattering.

IV. EXAMPLES OF MOLECULAR CROSS SECTIONS

In this section some typical examples of the molecular cross sections are shown. The nuclear scattering amplitudes given in Refs. [3–8] are used as the input for computation of the molecular differential cross sections. These amplitudes are first averaged over the internal motion of nuclei inside the target molecules, according to Eq. (29). In Figs. 5 and 6, the averaged nuclear amplitudes $\overline{f_{11}^{1/2}}$ for the elastic scattering $p\mu(F{=}0)+\text{H}_2$ and $t\mu(F{=}0)+\text{T}_2$ are shown. The input nuclear amplitudes $f_{11}^{1/2}$ are plotted versus collision energy ε in the molecular c.m.s., using the high-energy asymptotic relation $\varepsilon = (\mathcal{M}/\mu_b)\varepsilon_b$. The cusp in the elastic cross section $p\mu + p$, located at the spin-flip threshold, is smeared out after the averaging over proton motion in H_2. Although the vibrational quantum for T_2 is smaller than that for H_2, smoothing of the amplitude for $t\mu + t$ elastic scattering is also important, owing to strong changes of its value within the energy interval of 0.1 eV. This is particularly visible in the cusp region and at $\varepsilon \to 0$. This smearing strongly affects the molecular cross sections, which are expressed by the squared ampli-

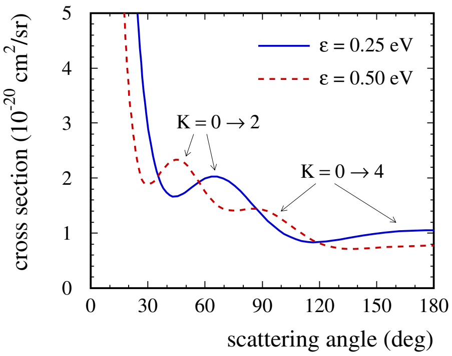

FIG. 7. (Color online) Differential cross section for $p\mu(F{=}0)$ scattering from a $\text{H}_2(K{=}0)$ molecule vs scattering angle ϑ.

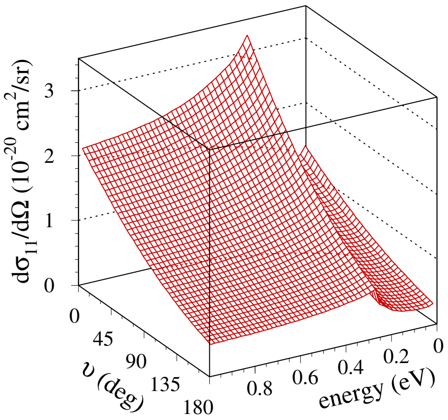

FIG. 8. (Color online) Doubled differential cross section for $p\mu(F=0)+p$ scattering vs ε and ϑ.

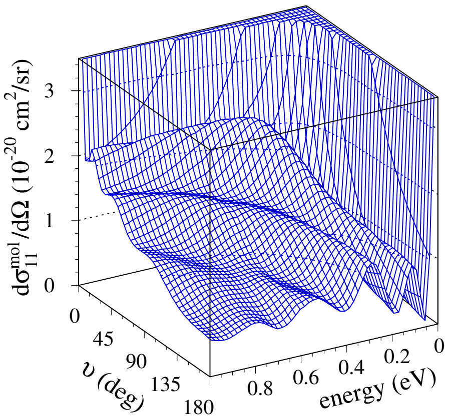

FIG. 9. (Color online) Differential cross section for $p\mu(F=0)+\mathrm{H}_2(K=0)$ scattering vs ε and ϑ.

tudes. The elastic cross sections for $d\mu+d$ scattering are quite flat at the lowest energies [3,5,6]. As a result, differences between the amplitudes f_{if}^S and $\overline{f_{if}^S}$ are much smaller than in the protium or tritium case. The role of smearing effects was investigated during a final analysis of the Abbott *et al.* diffusion data [16]. A spectacular improvement of the fits to the data, especially for $p\mu$ diffusion in H_2, was achieved when the averaged nuclear amplitudes $\overline{f_{if}^S}$ were used for the calculations of the molecular cross sections. This mainly concerns the elastic cross sections, as smoothing effects are generally much smaller in the case of spin-flip or isotopic-exchange amplitudes, which weakly depend on the energy below 1 eV [3–5,7,8].

Electron-screening and molecular-binding effects are clearly seen in the molecular differential cross sections. The range of the screening potential (54) is on the order of a_e, so that the condition $k_0 a_e \sim 1$ is satisfied already at $\varepsilon \sim 0.001$ eV. Many partial waves begin to contribute significantly to the screening amplitude (56) above 0.001 eV. As a result, the molecular cross sections are anisotropic even at very low energies. Moreover, scattering from a molecule is connected with different rotational transitions, which additionally leads to a complicated angular distribution of the scattered atoms. This is in contrast to $a\mu$ scattering from a bare hydrogen nucleus, where few partial waves contribute significantly to the nuclear cross sections below 100 eV. In all of the three-body cases, the s-wave cross section describes scattering below 0.1–1 eV well, which is therefore isotropic in the nuclear c.m.s. The cross section $d\sigma_{0n}/d\Omega$ for $p\mu$ scattering from a ground-state H_2 molecule is presented in Fig. 7, for $\varepsilon=0.25$ and 0.5 eV. Scattering at the angle $\vartheta \lesssim 30°$ is dominated by $p\mu$ scattering from the electron cloud. The peaks at greater angles are due to the rotational transitions $K=0\rightarrow K'=2$ and $K=0\rightarrow K'=4$. The angular positions of the scattering peaks change with the variation of $p\mu$ energy.

The differential cross sections for $p\mu$ scattering from a free proton and from a H_2 molecule are plotted in Figs. 8 and 9 as functions of the collision energy ε and the scattering angle ϑ in the molecular c.m.s. Figure 8 illustrates the cross section for the elastic $p\mu+p$ scattering, multiplied by 2. The mass of the target particle is, however, set to the H_2 mass, for the sake of comparison with this molecular target. Only the s wave contributes to the $p\mu+p$ cross section in the considered energy interval. However, the scattering is not isotropic in the molecular c.m.s. A cusp is apparent at the energy of the spin-flip threshold. The surface in Fig. 9 describes the corresponding cross section $d\sigma_{0n}/d\Omega$ (cut above a value of 3.5×10^{-20} cm^2/sr) for the ground-state H_2 molecule. The electron-screening contribution to the differential cross section is clearly seen at all angles for $\varepsilon \lesssim 0.05$ eV and only as a forward peak at higher energies. The lowest rotational transitions can be distinguished in this plot. Also a smearing of the molecular cross section due to the proton internal motion in H_2 is visible, especially in the spin-flip threshold region. The sections of the surfaces shown in Figs. 8 and 9 with the plane $\varepsilon=1$ eV are already quite similar, apart from the forward scattering. Thus, the molecular scattering at larger energies and angles, which contains contributions from many rotational-vibrational transitions, approaches the "doubled" nuclear scattering. For a better comparison, the angular dependence of the doubled nuclear and the molecular cross sections are shown in Figs. 10 and 11, at a fixed collision energy. For $\varepsilon=0.1$ eV, the two cross sections are very different at all angles. For $\varepsilon=1$ eV, these cross sections are already quite similar at larger angles $\vartheta \gtrsim 20°$. One sees that there are only small rotational oscillations of the molecular curve around the doubled nuclear curve.

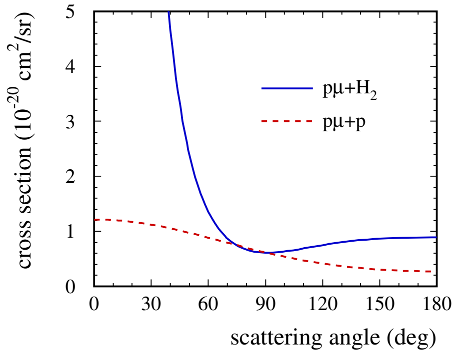

FIG. 10. (Color online) Angular dependence of the differential cross sections for $p\mu(F=0)$ scattering on a proton (doubled) and on $\mathrm{H}_2(K=0)$, at $\varepsilon=0.1$ eV.

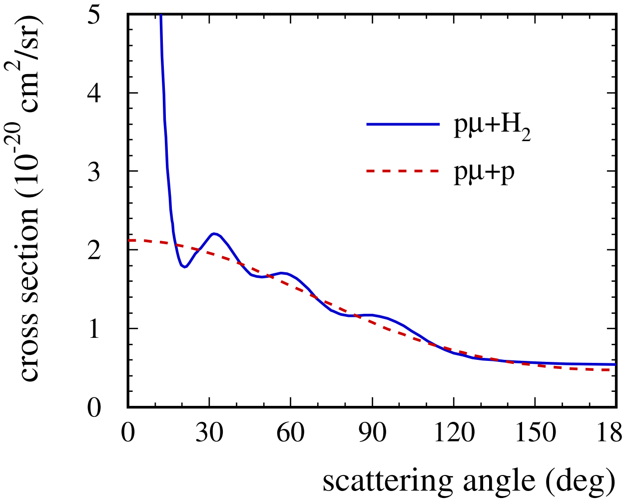

FIG. 11. (Color online) The same as in Fig. 10, at $\varepsilon = 1$ eV.

The differential cross sections for the downwards spin-flip reaction in $p\mu(F=1)$ scattering from a proton and from a H_2 molecule are shown in Figs. 12 and 13. Electron-screening and molecular-binding effects in the spin-flip reactions are not so important as in the case of spin-conserving scattering (cf. Figs. 9 and 13), owing to higher momentum transfers. Larger differences between the nuclear and the molecular spin-flip cross sections appear mainly at small collision energies and small angles.

Simulations of experiments performed in gaseous hydrogenic targets require knowledge of the differential cross sections for the molecular processes (1). These molecular cross sections have been computed and stored as computer files. They have been applied for planning and interpreting many experiments in H-D gaseous targets. For example, optimal conditions for studies of μ^- nuclear capture in $p\mu$ [11,12] and for the measurement of the Lamb shift in $p\mu$ atoms [13–15] created in H_2 targets have been determined using the calculated molecular cross sections. These experiments are now under way.

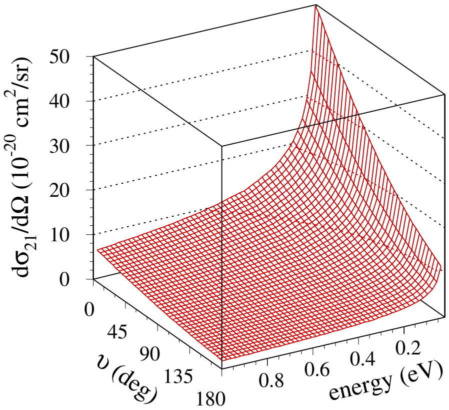

FIG. 12. (Color online) Doubled differential cross section for the downward spin-flip reaction in $p\mu(F=1)$ scattering from a proton vs ε and ϑ.

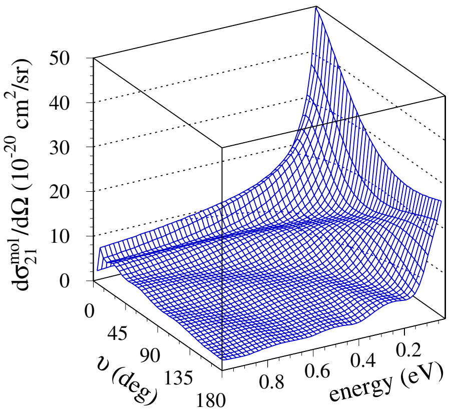

FIG. 13. (Color online) Differential cross section for the downward spin-flip reaction in $p\mu(F=1)$ scattering from $H_2(K=0)$ vs ε and ϑ.

V. CONCLUSIONS

A method of calculating the differential cross sections for low-energy muonic-atom scattering from hydrogenic molecules has been developed. This method directly uses the corresponding amplitudes for muonic-atom scattering from hydrogen-isotope nuclei, calculated within the framework of the adiabatic method for the three-body problem with the Coulomb interaction. Thus, the presented method naturally includes the angular and energy dependence of the three-body amplitudes in the scattering from hydrogenic molecules. Since, in many cases, the considered three-body scattering amplitudes depend strongly on the collision energy within the interval $\lesssim 0.1$ eV, a broad distribution of the nucleus kinetic energy in a hydrogenic molecule is taken into account. The molecular vibrations are described in the harmonic approximation. Therefore, the evaluated cross sections are valid below a few eV.

For a fixed energy ε of a muonic atom collision with a hydrogenic molecule, the calculated collision energy ε_b in the system consisting of the atom and a single hydrogen-isotope nucleus has a wide spectrum. At $\varepsilon \to 0$, this spectrum reveals the shape of the kinetic energy distribution of the nucleus in a given rotational-vibrational state of the molecule. This effect is very significant, even for the molecular ground state, as the energy of zero-point vibration in hydrogenic molecules is quite large. The width of the ε_b spectrum for the lightest H_2 molecule is on the order of 0.1 eV. At higher ε, this width is even larger. As a result, the three-body amplitudes are strongly smoothed when calculating the molecular cross sections. This effect and the energy and angular dependence of the three-body amplitudes are included in the calculated set of differential cross sections for low-energy scattering of 1S muonic hydrogen atoms from hydrogenic molecules. These theoretical cross sections give good agreement with many experiments involving $p\mu$ and $d\mu$ scattering in gaseous H-D targets. The presented method can also be applied for scattering of other ground-state exotic atoms or neutrons from hydrogenic targets.

[1] S. I. Vinitsky and L. I. Ponomarev, Fiz. Elem. Chastits At. Yadra **13**, 1336 (1982) [Sov. J. Part. Nucl. **13**, 557 (1982)].

[2] V. S. Melezhik, L. I. Ponomarev, and M. P. Faifman, Zh. Eksp. Teor. Fiz. **85**, 434 (1983) [Sov. Phys. JETP **58**, 254 (1983)].

[3] M. Bubak and M. P. Faifman, JINR, Dubna, Technical Report No. E4-87-464, 1987 (unpublished).

[4] L. Bracci *et al.*, Phys. Lett. A **134**, 435 (1989).

[5] L. Bracci *et al.*, Muon Catal. Fusion **4**, 247 (1989).

[6] L. Bracci *et al.*, Phys. Lett. A **149**, 463 (1990).

[7] A. Adamczak *et al.*, Phys. Lett. B **285**, 319 (1992).

[8] C. Chiccoli *et al.*, Muon Catal. Fusion **7**, 87 (1992).

[9] W. H. Breunlich, P. Kammel, J. S. Cohen, and M. Leon, Annu. Rev. Nucl. Part. Sci. **39**, 311 (1989).

[10] L. I. Ponomarev, Contemp. Phys. **31**, 219 (1990).

[11] P. Kammel *et al.*, Nucl. Phys. A **663-664**, 911c (2000).

[12] P. Kammel *et al.*, Hyperfine Interact. **138**, 435 (2001).

[13] F. Kottmann *et al.*, Hyperfine Interact. **138**, 55 (2001).

[14] R. Pohl *et al.*, Hyperfine Interact. **138**, 35 (2001).

[15] R. Pohl *et al.*, Can. J. Phys. **83**, 339 (2005).

[16] D. J. Abbott *et al.*, Phys. Rev. A **55**, 214 (1997).

[17] E. Fermi, Ric. Sci. **7**, 13 (1936).

[18] G. Breit, Phys. Rev. **71**, 215 (1947).

[19] B. A. Lippmann and J. Schwinger, Phys. Rev. **79**, 469 (1950).

[20] S. W. Lovesey, *Theory of Neutron Scattering from Condensed Matter* (Clarendon Press, Oxford, 1984).

[21] J. A. Young and J. U. Koppel, Phys. Rev. **135**, A603 (1964).

[22] A. Adamczak, Muon Catal. Fusion **4**, 31 (1989).

[23] A. Adamczak, Hyperfine Interact. **82**, 91 (1993).

[24] N. F. Mott and H. S. W. Massey, *The Theory of Atomic Collisions* (Clarendon Press, Oxford, 1965).

[25] K. Huang and C. N. Yang, Phys. Rev. **105**, 767 (1957).

[26] R. Stock, A. Silberfarb, E. L. Bolda, and I. H. Deutsch, Phys. Rev. Lett. **94**, 023202 (2005).

[27] A. Boukour, V. S. Melezhik, and C. Leclercq-Willain, Phys. Rev. A **60**, 323 (1999).

[28] J. S. Cohen, Phys. Rev. A **44**, 2836 (1991).

[29] A. Adamczak and V. S. Melezhik, Phys. Lett. A **118**, 181 (1986).